

Anodically electrodeposited Co + Ni mixed oxide electrode: preparation and electrocatalytic activity for oxygen evolution in alkaline media

Gang Wu^{a,*}, Ning Li^b, De-Rui Zhou^b, Kurachi Mitsuo^c, Bo-Qing Xu^a

^a*Innovative Catalysis Program, Key Lab of Organic Optoelectronics & Molecular Engineering, Department of Chemistry, Tsinghua University, Beijing 100084, China*

^b*Department of Applied Chemistry, Harbin Institute of Technology, Harbin 150001, China*

^c*Faculty of Engineering, Kyoto University, Kyoto 606-8283, Japan*

Received 5 March 2004; received in revised form 6 June 2004; accepted 9 June 2004

Available online 21 August 2004

Abstract

Co + Ni mixed oxides on Ni substrate were prepared through anodic electrodeposition from $\text{Co}(\text{NO}_3)_2$ and $\text{Ni}(\text{NO}_3)_2$ aqueous solutions with five different $\text{Co}^{2+}/\text{Ni}^{2+}$ ratios beside only Co^{2+} . By the electrochemical measurements, the optimum performance in electrocatalytic activity for oxygen evolution reaction in alkaline media was obtained on the Co + Ni mixed oxide deposited from the solution containing $\text{Co}^{2+}/\text{Ni}^{2+}$ ratio of 1:1. The mixed oxide is corresponding to about 68 at% Co contents with spinel-type NiCo_2O_4 phase and porosity surface structure. The electrochemical kinetic parameters including exchange current density, Tafel slopes, reaction order with respect to $[\text{OH}^-]$ and standard electrochemical enthalpy of activation were analyzed also. A possible mechanism involving the formation of a physisorbed hydrogen peroxide intermediate in a slow electrochemical step was presented, which accounts for the values of the experimental results.

© 2004 Elsevier Inc. All rights reserved.

Keywords: Mixed oxide; Cobalt oxide; Nickel oxide; Anodic electrodeposition; Oxygen evolution; Electrocatalysis

1. Introduction

Oxygen electrode reactions play an important role in electrochemical science and technology because they are involved in many electrochemical systems like water electrolyzer, fuel cells, metal-air batteries, sensors, etc. At present, due to the high overpotential of oxygen evolution reactions (OER), alkaline water electrolysis normally shows low energy efficiency and much efforts have been directed to the study of transition metal oxides as oxygen evolving anodes in alkaline media, in an attempt to lower the overpotential.

Oxides constitute a wide class of materials with good electrocatalytic activity for many electrode reactions, for

example, O_2 evolution, O_2 reduction, and organic electrosynthesis [1–3]. Tseung [4] and Trasatti [5] put forward guidelines for the choice of semiconducting oxides for the oxygen evolution reaction. They emphasized that oxygen evolution can only proceed when the electrode potential is higher than the potential of the metal/metal oxide couple or the lower metal oxide/higher metal oxide couple. Thus the ideal couple will be the one which has potential lower or similar to the theoretical potential of the oxygen evolution reaction. Moreover the criteria for choosing mixed oxide electrode material for an industrial application, which is based mostly on a compromise between electrocatalytic activity, long-term stability and cost, have led to the development of new anode materials. However, the range of improvement of the activity of a mono-oxide is rather limited. So mixed oxides are used to modulate the

*Corresponding author. Fax: +86-10-6279-2122.

E-mail address: wugang@mail.tsinghua.edu.cn (G. Wu).

electrode properties through synergetic effects arising from the intimate electronic interaction of the components [6,7].

Synergetic effects are possible as two or more oxides are mixed together. For these reasons, studies of mixed oxides for electrochemical applications are rather common [8–11]. Ni and Co oxides exhibit interesting electrocatalytic activities, which make them attractive for O₂ evolution [12,13]. For instance, in cobaltite spinels (MCo₂O₄), the mixed valences of the cations are helpful in the reversible adsorption of oxygen by providing donor–acceptor sites for chemisorptions. Co₃O₄ and NiCo₂O₄ has long been known to be an active and stable bifunctional catalyst for oxygen evolution and reduction in alkaline media, as well as a catalyst in alcohol and amine electro oxidation [14–16]. So the investigation of the electrocatalytic synergism of Ni + Co mixed oxides has attracted considerable attention in view of their potential applications in electrocatalysis. Actually these mixed oxides can be prepared by diverse techniques like sputtering, thermal decomposition, immersion processes. S. Trasatti et al. [17] studied the surface properties of Ni + Co mixed oxides prepared through thermal decomposition of nitrates by X-ray diffraction (XRD), X-ray photoelectron spectroscopy (XPS), Brunauer–Emmett–Teller (BET) adsorption, and point of zero charge (PZC) methods. King and Tseung [13] prepared mixed oxides of five compositions between the mono-Ni and mono-Co oxides including the stoichiometric compounds NiCo₂O₄ and Ni₂CoO₄. The oxides were prepared by thermal decomposition of mixtures of the respective nitrates, used as precursors, at 300 °C for 24 h. The mixtures were obtained by the method of freeze-drying. The maximum electrocatalytic activity for O₂ reduction was observed in the spinel NiCo₂O₄. However, the results from Gennero [18] and Wen [19], indicated the maximum activity of oxygen evolution reaction was observed on the Ni + Co mixed oxides with about 50 mol% Ni, prepared by thermal decomposition of nitrates at 360–400 °C on Ni and Ti substrate, respectively. By the Sol–gel technique at 150–400 °C, Serebrenikova and Birss [20] have prepared Ni and Co oxide films on polycrystalline structure Pt. Only the mixed oxide with equimolar composition has been studied besides the mono-oxides. The mixed oxide exhibits a higher activity than the mono-oxides. The structure and the phase diagram of Ni and Co mixed oxides have been investigated.

Besides the thermal decomposition and sol–gel techniques, transition metal oxide/hydroxide films can be formed by electrochemical growth on the corresponding metals. Tench and Warren [21] reported their results describing a general technique for the electrochemical deposition of oxide/hydroxide films of nickel, cobalt, copper, iron and manganese from aqueous solutions. The electrochemical technique may be envisaged as a

possible way of preparing active oxide films and offers a number of unique advantages in comparison to other procedures. For instance, very thin and homogeneous films with specific morphological and chemical properties can be prepared. The physical properties of the relevant deposits can be easily modulated by means of the various experimental parameters affecting the electrodeposition process such as electrolyte composition, pH, applied potentials, deposition time and electrode substrate. By this technique, Chen and Noufi [22] had prepared mono-nickel and mono-cobalt oxide on platinum and graphite electrodes and investigated their activity for oxygen evolution reaction. The results showed the Ni(III) oxide had good electrocatalytic activity and long-term stability for oxygen evolution, however the Co(III) oxide showed initial decay during an extensive electrolysis. In addition, recently several papers have appeared on this subject, describing the electrodeposition techniques for preparing CoO_x [23,24] and MnO₂ + WC [25] composite electrodes for oxygen evolution. However, as we know, preparing mixed oxides by electrochemical technique is scanty. In particular there is no detailed study of the catalytic activity as a function of composition in Co + Ni mixed oxides.

In this work, anodically electrodeposited Co + Ni mixed oxides films through potential cycling in solutions containing five different Co²⁺/Ni²⁺ ratios, besides mono-Co oxide, were characterized by XRD, AFM and different electrochemical methods. The kinetics and mechanism of the OER on Co + Ni mixed oxides in alkaline solutions were also investigated.

2. Experimental details

2.1. Preparation of the oxides by potentiodynamic electrodeposition

Co + Ni mixed oxides were prepared by anodic electrodeposition in 1 M NaOH electrolytes, which contain different concentration of Co(NO₃)₂·6H₂O and Ni(NO₃)₂·6H₂O and 0.5 M glycol. Five different Co²⁺/Ni²⁺ mole ratios (a) 5:1; (b) 2:1; (c) 1:1; (d) 1:2 and (e) 1:5, which total metal ions concentration equal to 0.01 M, were used. For the sake of comparison, the only Co²⁺ solution was applied to obtain mono-Co oxide. Electrodeposition was performed in three-compartment cells under nitrogen gas saturation and a temperature of 25 °C. Nickel plates (99.7%, 1 cm × 2 cm × 0.025 cm), were used for substrates as the working electrodes. Prior to the anodic deposition, the surface of nickel was degreased and immersed in 10 wt% H₂SO₄ at room temperature for 60 s. Another sheet of nickel of large area was used as counter electrode and Hg/HgO/1 M OH⁻ electrode as reference

electrode. Solution was stirred with a magnetically driven Teflon coated stirring bar. The potential in anodic electrodeposition involves repetitive triangular potential scans (RTPS) [23]. Prior to the RTPS, the electrode was polarized at $E = -1.2$ V for 5 min to reduce air formed films on nickel plates. The working electrode was subject to RTPS, between $E_{sc} = -0.1$ V and $E_{sa} = 0.7$ V, at $v = 0.05$ Vs⁻¹ for 4 h, $\omega = 100$ rpm. After electrodeposition the working electrodes were rinsed with double distilled water and dried in 80 °C for 2 h. All potentials are given relative to the standard hydrogen electrode (SHE).

2.2. Surface composition and crystalline structure of mixed oxides

X-ray photoelectron spectroscopy (XPS) was employed to study the surface composition of the electrodeposited mixed oxides. XPS measurements were performed using an ESCA 3 Mark II instrument, with MgK_α X-ray radiation as the excitation source. XPS core spectra were collected for Ni2p and Co2p shells.

The anodically deposited mixed Co+Ni oxide films were measured by X-ray diffraction (XRD) recorded by a Bede D1 diffractometer, starting from $2\theta = 15^\circ$ to 85° in 0.05° and 1 s steps. The CuK α ray ($\lambda = 0.15418$ nm) was selected through a graphite monochromator. The incident beam reached the sample with an incident angle of about 2° . The main advantage of this setup is that allow the incident beam to cross a surface thickness from 200 to 1000 nm. The mixed oxide films were examined by atomic force microscopy (AFM) (Nanoscopy IIIa) to investigate surface roughness and microstructure.

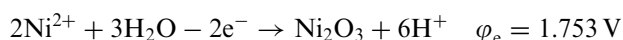
2.3. Electrochemical measurements

The electrochemical behaviors of mixed Co+Ni oxides for oxygen evolution reaction were characterized by different electrochemical measurements in 1 M NaOH solutions. Cyclic voltammograms were run between -0.1 and 0.65 V. Steady-state Tafel polarization and electrochemical impedance spectroscopy (EIS) were used to study the kinetics of oxygen evolution reaction. Steady-state Tafel polarization and cyclic voltammetric measurements were performed with an EG&G M273 potentiostat. Electrochemical impedance measurements were performed using the above-mentioned potentiostat and a Solartron SI 1255 HF frequency response analyzer. The data obtained from impedance measurements were analyzed by nonlinear least squares fit (NLLS) routine.

3. Results

3.1. Preparation of Co+Ni mixed oxide electrodes

In order to obtain efficient electrodeposition of Co+Ni mixed oxide species, an electrolytic medium must be selected in which the low-valence metal (i.e., Co(II) and Ni(II)) is soluble, while the corresponding high-valence oxides (i.e., Co(III), Co(IV), Ni(III) and Ni(IV)) are insoluble. Nevertheless, in general the Co(III) or Ni(III) oxide species are soluble at $\text{pH} < 7$ and Co(II) and Ni(II) cation species gives rise to insoluble compounds at $\text{pH} > 7$. Thus, in order to attempt electrodeposition of Co+Ni mixed oxides on substrate, a neutral medium seems to provide the best conditions for success. However, from the literature [26], the reactions and their standard electrode potential about oxidation of Co²⁺ and Ni²⁺ to higher valent oxides in neutral medium are as follow:



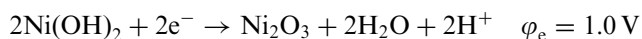
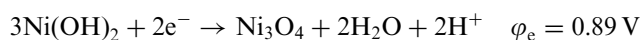
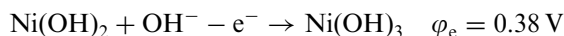
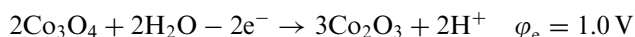
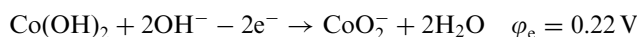
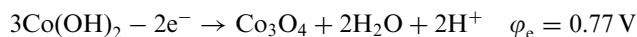
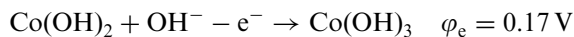
So it can be seen only at very higher potential (> 1.5 V), Co²⁺ and Ni²⁺ can be oxidized to high valent oxides. Furthermore, Co and Ni oxide-based materials, when used as heterogeneous catalysts, show good chemical stability and electroactivity only in alkaline conditions. Therefore, studies regarding novel methods for preparing Co+Ni mixed oxide thin films directly in the alkaline medium are encouraged.

As we know, two ways can make the cobalt and nickel hydroxide keep stable. One is addition of complex ions such as citrate, tartrate and cyanide, the other way is production of colloid. In our experiments, to produce stable colloidal Co(OH)₂ and Ni(OH)₂, a little amount metal ions were added in solution with a large amount OH⁻ little by little to avoid precipitation. In addition, special amount polyol like glycol was added also to increase the stability and viscosity of solution. The increased viscosity of solution would be helpful to maintain the oxidized higher valent oxide on the substrate and not to be removed easily in flowing electrolytes.

The voltammetric behavior of the cobalt and nickel oxides in alkaline medium is rather complex, because several oxidation states of Co or Ni and different varieties of oxides species and their relevant allotropic phases such as M(OH)₂, MO, M₂O₃, M₃O₄, MO₂ (M=Co, Ni) are likely to be involved in the electrochemical processes. The relevant amounts of these

oxides are strictly dependent on the actual chemical and physical status of the electrode surface, composition of the electrolytic solution, polarization time and relevant values of the applied potentials [24].

The probably reactions is as follows [26]:



On each triangular potential scans, between $E_{sc} = -0.1 \text{ V}$ and $E_{sa} = 0.7 \text{ V}$, new M^{2+} is oxidized and deposited, and the oxide deposit is cycled between $M(\text{III})$ or $M(\text{IV})$ and $M(\text{OH})_2$.

Co+Ni mixed oxides prepared by this potential cycling technique appear to be uniform and good adherence. Based on the voltammetry peak charge, approximate calculation of the mixed oxide thickness is about $1 \mu\text{m}$ after a 4 h anodic electrodeposition, assuming a cubic lattice and $M\text{--O}$ bond distance of 4.2 \AA [21].

Fig. 1 shows the Co contents in mixed oxide films, by XPS, changing with $\text{Co}^{2+}/\text{Ni}^{2+}$ ratios in solutions for anodic electrodeposition. The result indicates that Co contents in mixed oxide film increase with $\text{Co}^{2+}/\text{Ni}^{2+}$

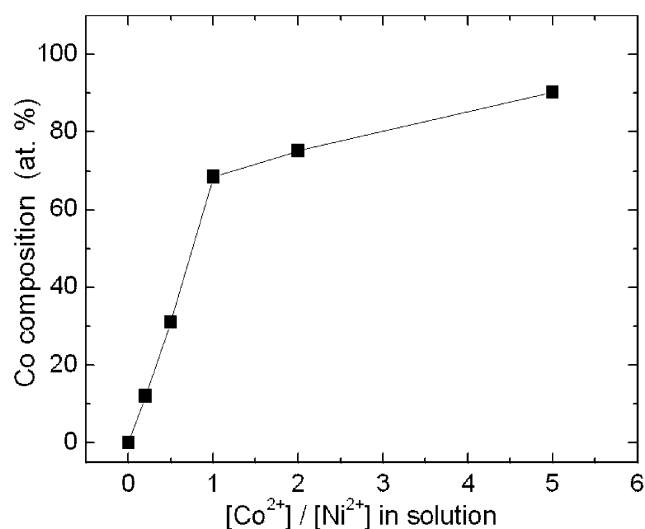


Fig. 1. Co contents in mixed oxides obtained by XPS as a function of Co^{2+} proportion in solutions during the process of anodic electrodeposition.

ratios. Moreover, Co contents in films are always higher than that in solutions. A reasonable explanation why the electrodeposition rate from Co^{2+} to Co^{3+} is faster than that from Ni^{2+} to Ni^{3+} is as follow:

The standard equilibrium transition potential φ_e of $\text{Co}(\text{II})/\text{Co}(\text{III})$ is about ca. 0.17 V and more negative than that of $\text{Ni}(\text{II})/\text{Ni}(\text{III})$ ($\varphi_e = 0.38 \text{ V}$) [26]. From the point of electrochemical kinetic, the reaction rate can be expressed by anodic current density j_a . When the reaction rate is controlled by electrochemical step, then:

$$j_a = FK C_{M^{2+}} \exp\left[\frac{\alpha n F}{RT} (\varphi - \varphi_e)\right], \quad (1)$$

where $C_{M^{2+}}$ is the metal ion concentration, φ_e the equilibrium electrode potential, and φ the reaction electrode potential. When the reaction rate is controlled by diffusion step, then

$$j_d = FD_M \frac{dC_M}{dX}$$

where D_M is diffusion coefficients of metal ion.

So whichever the electrochemical step or diffusion step is control step, there are three main factors that affect anodic electrodeposition rate, such as electrode potentials, diffusion coefficients and relative concentrations. The diffusion coefficient can be determined by ion radius when the temperature and viscosity of solution are constant. The diffusion coefficient of Ni^{2+} and Co^{2+} is almost similar, due to their similar ion radius. Moreover when $\text{Co}^{2+}/\text{Ni}^{2+} = 1:1$, the concentration of metal ions is same. So from the above analysis, the only different factor between Co^{2+} and Ni^{2+} is the $\varphi - \varphi_e$. At identical oxidation potential φ , the $\varphi - \varphi_e$ of $\text{Co}(\text{II})/\text{Co}(\text{III})$ is larger than that of $\text{Ni}(\text{II})/\text{Ni}(\text{III})$. So we can think the $\varphi - \varphi_e$ is main factor to cause the different deposition rate between Ni^{2+} and Co^{2+} .

Fig. 2 is the relationship between mixed oxides electrodeposited from different $\text{Co}^{2+}/\text{Ni}^{2+}$ ratio solutions and current density of OER on these oxides. It can be seen that the catalytic activity on the oxide from the different $\text{Co}^{2+}/\text{Ni}^{2+}$ ratio solution, goes through a maximum value, and then drops with increasing of cobalt contents. According to the results of Fig. 1, the mixed oxide from solution with $\text{Co}^{2+}/\text{Ni}^{2+}$ ratio of 1:1 corresponds to 68at% cobalt contents in deposits and shows the highest catalytic activity.

3.2. Structural characterization of mixed oxides

X-ray diffraction corresponding to the mixed oxides obtained from solutions with different $\text{Co}^{2+}/\text{Ni}^{2+}$ ratios are depicted in Fig. 3.

The X-ray diffraction spectrum corresponding to the oxide deposited from solution with only Co^{2+} (Fig. 3(a)) indicates that a well-crystallized phase is formed on the Ni substrate. Some peaks may be readily attributed to a

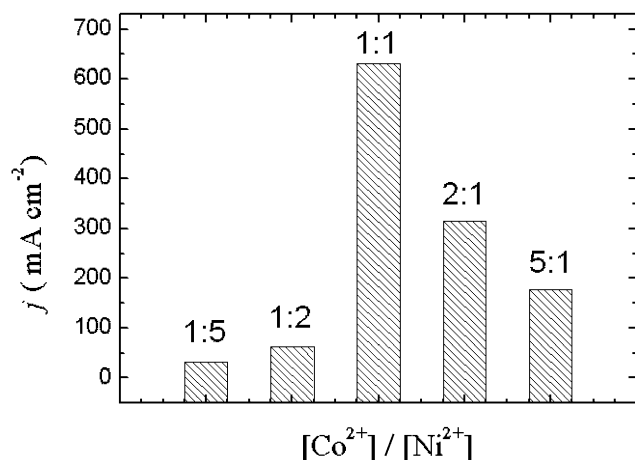


Fig. 2. The current density of OER at $E = 0.75$ V on the different Co+Ni oxides electrodeposited from solutions containing different $\text{Co}^{2+}/\text{Ni}^{2+}$ ratios.

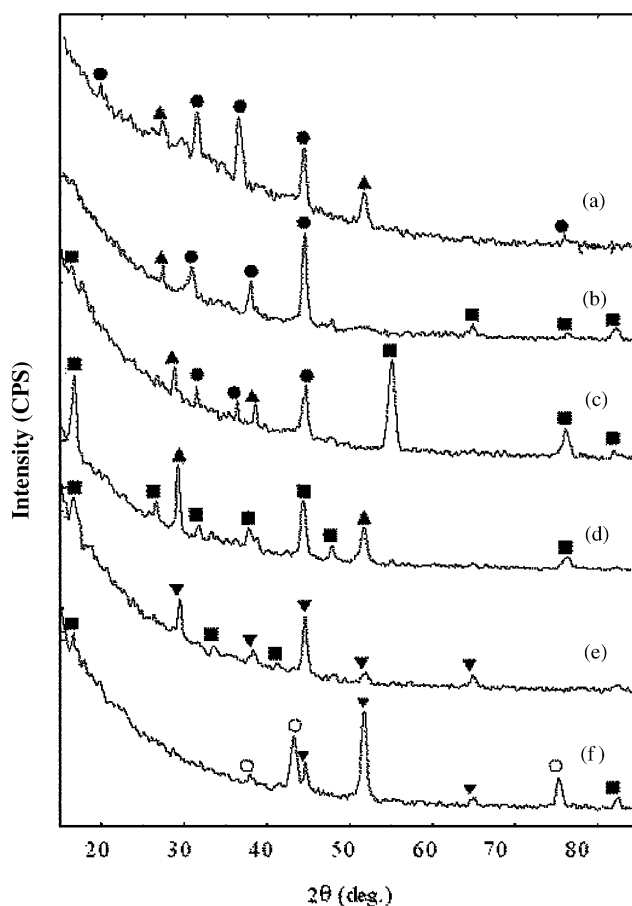


Fig. 3. X-ray diffraction patterns of Co+Ni mixed oxides electrodeposited from different $\text{Co}^{2+}/\text{Ni}^{2+}$ ratio solutions. (a) Only Co^{2+} , (b) 5:1, (c) 2:1, (d) 1:1, (e) 1:2, (f) 1:5; (●) Co_3O_4 ; (▲) Co_2O_3 ; (■) NiCo_2O_4 ; (▼) Ni_2O_3 ; (○) NiO .

spinel-type oxide Co_3O_4 , i.e., $2\theta = 19.796, 31.292, 36.872$ and 44.334 . In addition, the peaks corresponding to the Co_2O_3 phase are detected also. Figs. 3(b) and (c)

corresponding the mixed oxides from solutions with $\text{Co}^{2+}/\text{Ni}^{2+} = 5:1$ and $2:1$, respectively. Beside the peaks corresponding to the Co_3O_4 and Co_2O_3 phase, spinel NiCo_2O_4 phase may be readily observed. In Fig. 3(d), the mixed oxide deposited from solution containing $\text{Co}^{2+}/\text{Ni}^{2+} = 1:1$, exhibits the dominant diffraction spectrum corresponding to spinel-type NiCo_2O_4 phase, i.e., $2\theta = 16.69, 26.216, 31.754, 44.36$ and 75.935 . In Figs. 3(e) and (f), the diffraction spectrum show the Ni_2O_3 and NiO phase is main component, together with peaks related to the NiCo_2O_4 phase. As a matter of fact, NiCo_2O_4 has good conductivity and electrocatalytic activity to O_2 evolution. These would be a reasonable explanation why the oxide obtained from solution containing $\text{Co}^{2+}/\text{Ni}^{2+} = 1:1$ exhibits best electrocatalytic activity among different composition Co+Ni oxides, as shown in Fig. 2.

Fig. 4 shows AFM images of mixed Co+Ni oxide films deposited from solutions with different $\text{Co}^{2+}/\text{Ni}^{2+}$ ratios. Comparison of the AFM images of Co+Ni mixed oxides with different composition shows obvious differences in surface roughness and microstructure. The mixed oxide from solution with $\text{Co}^{2+}/\text{Ni}^{2+} = 1:1$ exhibits the highest surface roughness and real area, which contribute to decrease the overpotential and enhance catalytic performance for oxygen evolution reaction.

3.3. Electrocatalytic activity

3.3.1. CV curves characteristic

Fig. 5 present the cyclic voltammetry of mixed oxides, which were obtained from different $\text{Co}^{2+}/\text{Ni}^{2+}$ ratio solutions, in 1 M NaOH at a potential scan rate of 50 mV s^{-1} . Before cycling, the oxide electrodes were maintained at $+1.0$ V for 60 min, and no changes have been observed in the charge or the maximum current. The voltammograms were scanned between -0.1 and $+0.65$ V. Fig. 5(a) shows the voltammogram of oxide from solution with only Co^{2+} . The voltammogram exhibits two peaks in anodic process, at 0.20 and 0.35 V where the latter appears to be pronounced. This voltammogram is very similar to cyclic voltammograms corresponding to Co_3O_4 oxide with spinel structure prepared by spraying or sputtering on different substrate [27]. These peaks may be assigned to the $\text{Co(II)}/\text{Co(III)}$ and $\text{Co(III)}/\text{Co(IV)}$ redox processes. The reverse cathodic sweep shows a broad peak at about 0.22 V. Figs. 5(b)–(f), show the voltammetric behavior of the mixed Co+Ni oxides obtained from different $\text{Co}^{2+}/\text{Ni}^{2+}$ ratios (5:1, 2:1, 1:1, 1:2 and 1:5) by anodic electrodeposition, respectively. Due to the exchange potentials $\text{Co(III)}/\text{Co(IV)}$ and $\text{Ni(II)}/\text{Ni(III)}$ is very close to 0.35 V, so the anodic peaks appears in Figs. 5(b) and (c) at 0.18, 0.35 and 0.48 V, can be correlated to the $\text{Co(II)}/\text{Co(III)}$, $\text{Co(III)}/\text{Co(IV)}$, $\text{Ni(II)}/\text{Ni(III)}$ and $\text{Ni(III)}/\text{Ni(IV)}$. In Fig. 5(d), prior to the oxygen

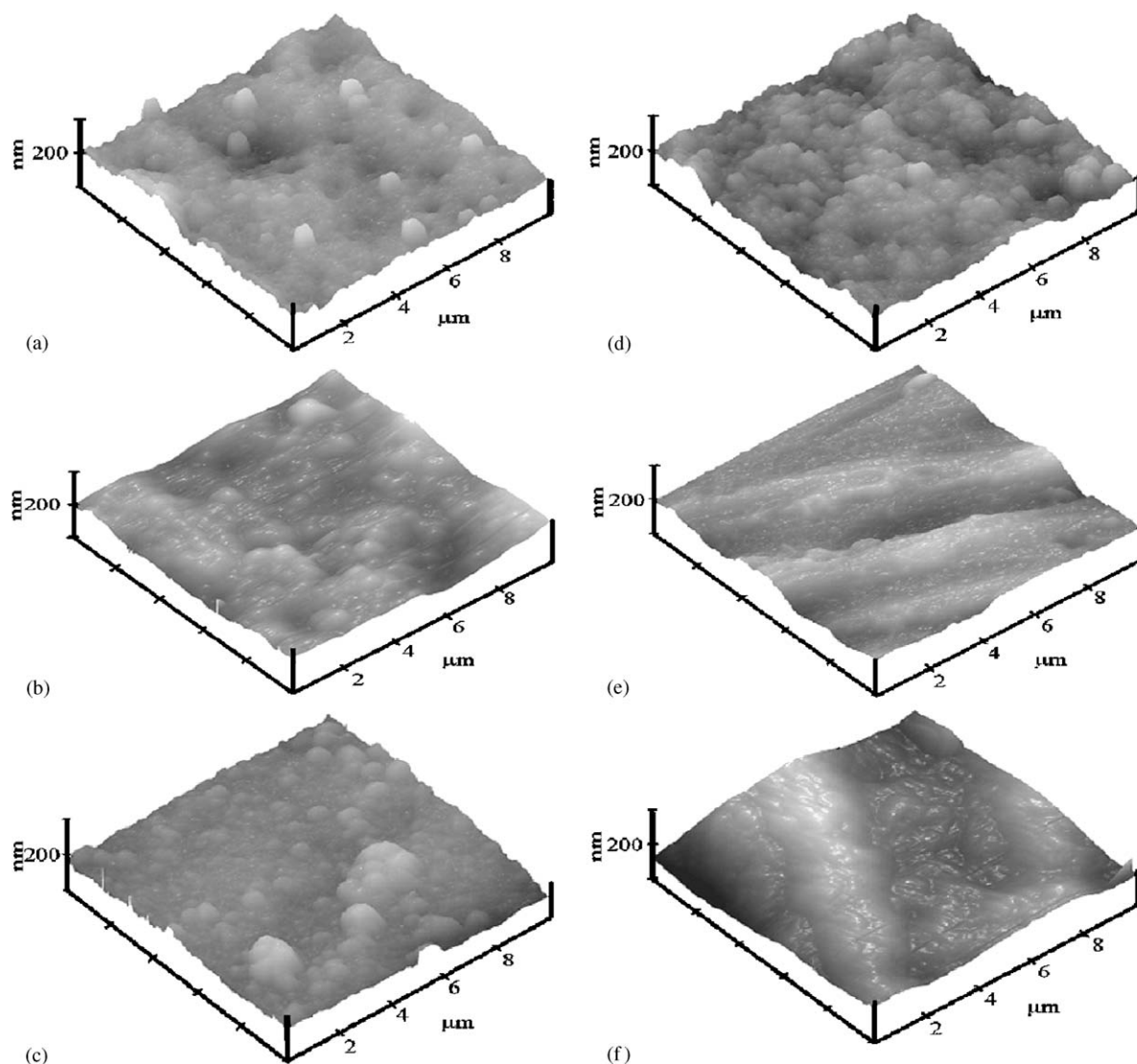


Fig. 4. AFM images of Co+Ni mixed oxides electrodeposited from different $\text{Co}^{2+}/\text{Ni}^{2+}$ ratio solutions. (a) Only Co^{2+} , (b) 5:1, (c) 2:1, (d) 1:1, (e) 1:2, and (f) 1:5.

evolution, two anodic peaks located at $E = 0.33$ and 0.45 V may be assigned to $\text{Co(III)}/\text{Co(IV)}$ and $\text{Ni(III)}/\text{Ni(IV)}$ transitions, respectively. The cathodic profile depicts a broad peak at 0.25 V corresponding to the reduction of Co(IV) , Ni(IV) species. Both Fig. 5(e) and Fig. 5(f) all show two anodic peaks at ca. 0.2 and 0.38 V, which were attributed to the transitions of $\text{Co(II)}/\text{Co(III)}$ and $\text{Ni(II)}/\text{Ni(III)}$. The negative shift of $\text{Ni(II)}/\text{Ni(III)}$ is attributed to the synergetic effect from the Co addition, which was reported to increase the activity and reversibility of the $\text{Ni(II)}/\text{Ni(III)}$ [28,29]. It can be noted from voltammograms that the oxide from solution containing $\text{Co}^{2+}/\text{Ni}^{2+}$ ratio of 1:1 has the largest charge densities of anodic peaks corresponding to the transitions of $\text{Co(III)}/\text{Co(IV)}$ and $\text{Ni(III)}/\text{Ni(IV)}$ and shows best electrocatalytic performance for OER.

3.3.2. Steady-state Tafel curves

The Tafel plots of OER on Co+Ni mixed oxide electrodes electrodeposited from different $\text{Co}^{2+}/\text{Ni}^{2+}$ ratio solutions are shown in Fig. 6. All polarization curves were corrected for ohmic drop effects, with resistance values obtained from impedance measurements. The corresponding kinetic parameters including exchange current density and Tafel slope are summarized in Table 1. From Fig. 6, it can be seen that the all Co+Ni mixed oxide electrodes show two well-defined Tafel regions i.e., $40\text{--}48$ mV dec^{-1} at low overpotential region and $110\text{--}120$ mV dec^{-1} at high-overpotential region. Such a behavior of Tafel line probably is due to the exchange in the valence state of the active site of anode materials and the influence of higher valence oxides on OER. Moreover, such a behavior of Tafel line

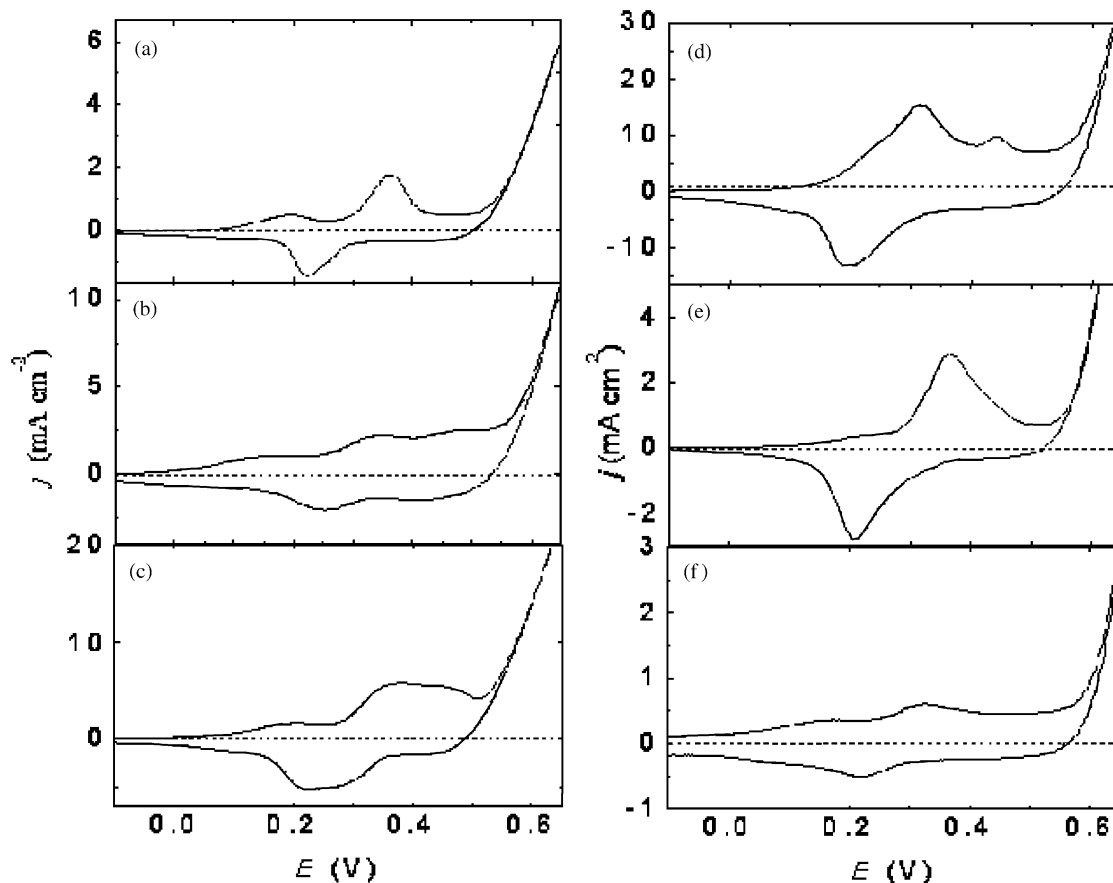


Fig. 5. Cyclic voltammetric behavior of Co + Ni mixed oxides electrodeposited from different $\text{Co}^{2+}/\text{Ni}^{2+}$ ratio solutions at a scan rate of 50 mV s^{-1} in 1 M NaOH (a) only Co^{2+} , (b) 5:1, (c) 2:1, (d) 1:1, (e) 1:2, and (f) 1:5.

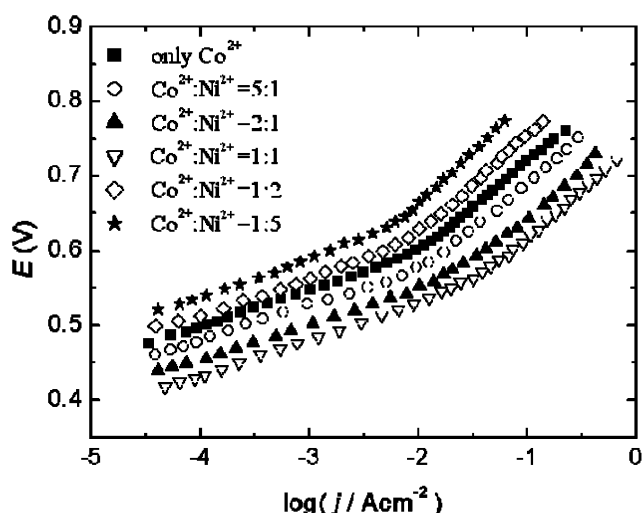


Fig. 6. Tafel plots for oxygen evolution reaction on the Co + Ni mixed oxides electrodeposited from different $\text{Co}^{2+}/\text{Ni}^{2+}$ ratio solutions, at 25°C . (■) Only Co^{2+} , (○) 5:1, (▲) 2:1, (▽) 1:1, (◇) 1:2, (★) 1:5.

is quite analogous to those reported for Ni and NiCo_2O_4 anodes for OER in alkaline medias [30]. From Table 1, it can be seen that among all mixed oxides, the mixed

oxide electrodeposited from 1:1 $\text{Co}^{2+}/\text{Ni}^{2+}$ ratio solution exhibits the highest j_0 value and the best catalytic performance for OER.

3.3.3. Apparent enthalpy obtained at different temperatures

The influence of temperature on the OER has been studied on all mixed Co + Ni oxides in 1 M NaOH and at 25, 35, 45, 55, 65°C . According to Eq. (2) [31], the standard apparent electrochemical enthalpy of activation, ΔH_{el} can be estimated by measuring the slope of the Arrhenius plot, $\log j$ vs. $1/T$, constructed at constant potential ($E = 0.60 \text{ V}$), chosen in the first Tafel region of the anodic polarization curves. The subscript E denotes constant potential

$$(\Delta H_{\text{el}})_E = -2.303R \left(\frac{\partial \log j}{\partial (1/T)} \right)_E \quad (2)$$

At 0.6 V, the current densities for the various oxide electrodes at different temperatures, express as A cm^{-2} were presented in Fig. 7. Values of the ΔH_{el} for the OER on different mixed Co + Ni oxide electrodes range between 39.2 and 51.7 kJ mol^{-1} (see Table 1) at $E = 0.60 \text{ V}$. It is noteworthy that the calculated activation enthalpy

Table 1
Kinetic parameters for oxygen evolution on Co+Ni mixed oxides electrodeposited from different $\text{Co}^{2+}/\text{Ni}^{2+}$ ratio solutions, in 1M NaOH, at 25 °C

$\text{Co}^{2+}/\text{Ni}^{2+}$	b (mV dec ⁻¹)		$10^6 j_0$ (A cm ⁻²)		ΔH_{el} (kJ mol ⁻¹)
	Low η	High η	Low η	High η	
Pure Co^{2+}	42.8	116.9	3.2	166	42.2
5:1	45.9	121.9	4.3	273	39.2
2:1	46.4	122.2	8.7	413	40.0
1:1	41.6	119.6	59	836	37.4
1:2	45.8	120.3	0.8	164	50.5
1:5	47.6	118.9	0.1	42	51.7

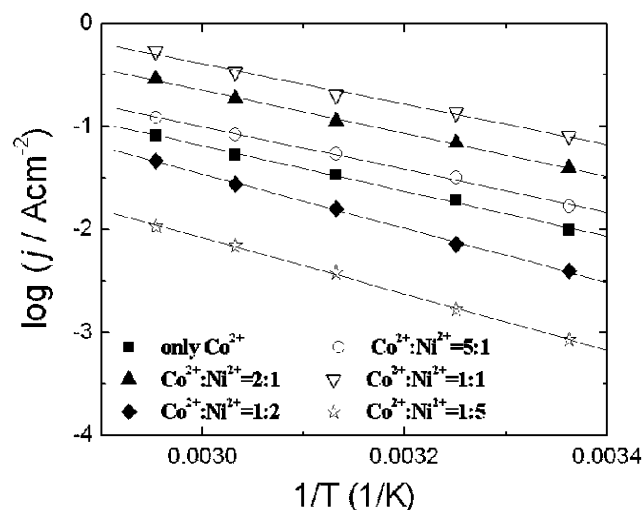


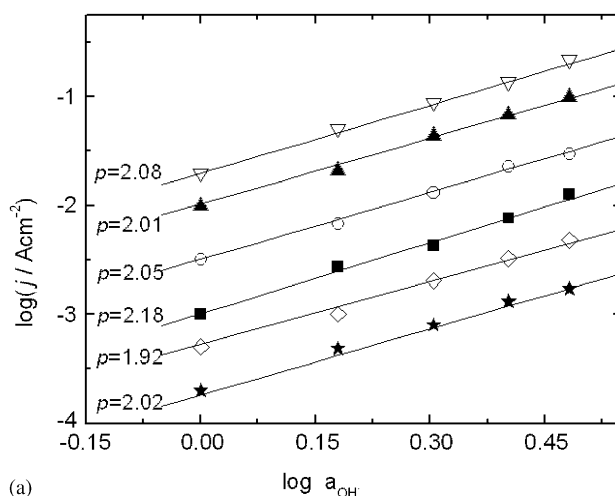
Fig. 7. Arrhenius plots for oxygen evolution on Co+Ni mixed oxides electrodeposited from different $\text{Co}^{2+}/\text{Ni}^{2+}$ ratio solutions, at $E = 0.6$ V. (■) Only Co^{2+} , (○) 5:1, (▲) 2:1, (▽) 1:1, (◆) 1:2, (☆) 1:5.

ΔH_{el} value for OER on the mixed oxide from solution of $\text{Co}^{2+}/\text{Ni}^{2+} = 1:1$ has the lowest value.

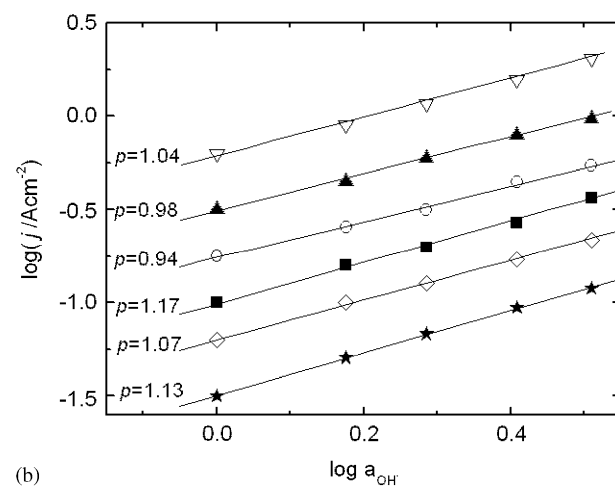
From the apparent current density of OER shown in Figs. 2 and 6, the mixed oxide with NiCo_2O_4 spinel phase deposited from $\text{Co}^{2+}/\text{Ni}^{2+} = 1:1$ solution has the best catalytic performance to OER. This result is the combination of the real activity and large specific area. However, the values of ΔH_{el} calculated from the plot slope of $\log j$ vs. $1/T$ and the factor of apparent area has been eliminated. So the values of the ΔH_{el} for the OER can reveal the real activity.

3.3.4. Reaction order with respect to $[\text{OH}^-]$

With the aim of obtaining the reaction order with respect to $[\text{OH}^-]$, the steady-state polarization curves of oxygen evolution on Co+Ni mixed oxides, were measured in $\text{NaNO}_3 + \text{NaOH}$ solutions with constant ionic strength (3 M) and variable NaOH concentration. Tafel slopes of mixed Co+Ni oxides almost keep constant within the whole OH^- concentration ranges



(a)



(b)

Fig. 8. Plots of $\log j$ versus $\log a_{\text{OH}^-}$ at constant potentials (a) $E = 0.55$ V; (b) $E = 0.72$ V and 25 °C, on Co+Ni mixed oxides electrodeposited from different $\text{Co}^{2+}/\text{Ni}^{2+}$ ratio solutions: (■) only Co^{2+} , (○) 5:1, (▲) 2:1, (▽) 1:1, (◇) 1:2, (★) 1:5, p is the plot slopes and denotes reaction order.

studied in this work, indicating no changes in the reaction mechanism of the OER. Plots of $\log j$ vs. $\log [\text{OH}^-]$ recorded at $E = 0.55$ and 0.72 V are depicted in Fig. 8. The reaction order p is the slope of the curve and was found to be close to 2.0 at low overpotential ($E = 0.55$ V), and to be close to 1.0 at high overpotential ($E = 0.72$ V). Reaction orders, with respect to OH^- , at low and high potential, close to 2.0 and 1.0, respectively, have also been reported for $\text{NiCo}_2\text{O}_4/\text{Ni}$ electrodes [32] and for spinel cobaltites [33] prepared by thermal decomposition.

3.3.5. EIS measurements for Co+Ni mixed oxides

In order to obtain mechanism information about the OER on Co+Ni mixed oxides, impedance measurements were performed in 1 M NaOH at 25 °C. Because the less satisfactory signal-to-noise ratio observable is

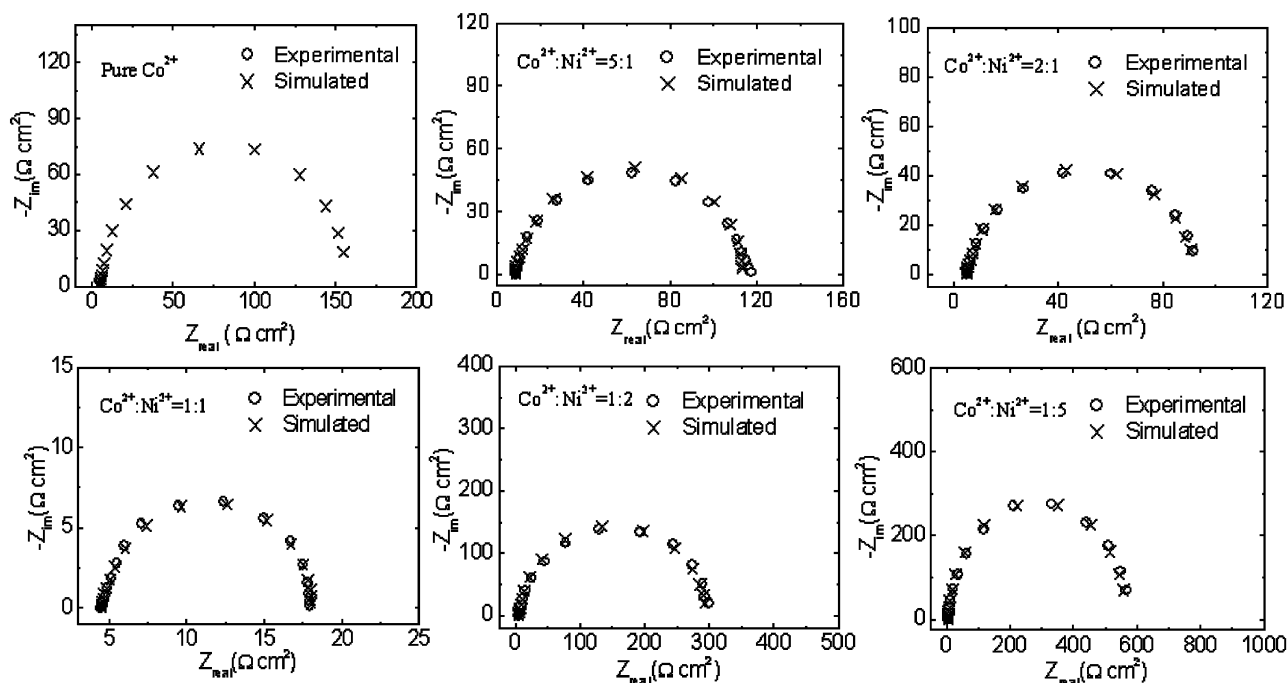


Fig. 9. Nyquist plots measured at $E = 0.58$ V corresponding to oxygen evolution reaction on the Co+Ni mixed oxides electrodeposited from different $\text{Co}^{2+}/\text{Ni}^{2+}$ ratio solutions, 1 M NaOH, 25 °C.

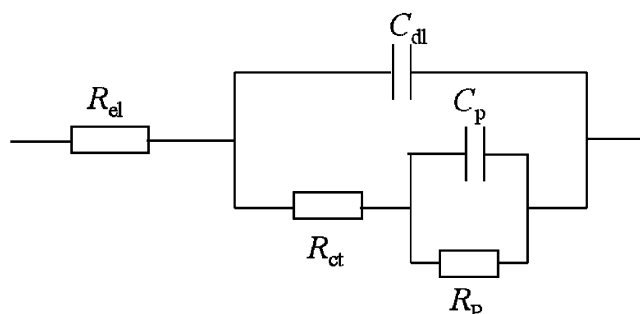


Fig. 10. Electrical equivalent circuit used for simulating the impedance spectra of oxygen evolution reaction on Co+Ni mixed oxides.

caused by the evolution of oxygen bubbles at higher overpotential, the chosen potential for impedance measurements is 0.58 V.

Impedance data corresponding to OER on mixed Co+Ni oxides are depicted in Fig. 9 and can be simulated by using the equivalent circuit shown in Fig. 10. Two overlapping capacitive loops may be detected, one of them being related to the interface double-layer capacitance C_{dl} , in parallel with the OER charge transfer resistance R_{ct} , the other one describing C_p and R_p . R_{ct} is charge transfer resistance of the electrode reaction and is the only circuit element that has a simple physical meaning describing how fast the rate of charge transfer during OER. R_{ct} also can be defined as

$$R_{ct} = \lim_{\omega \rightarrow 0} \text{Re}\{Z_f\},$$

where, $\text{Re}\{Z_f\}$ is real component in complex plots (Nyquist plots), ω is circular frequency $\omega = 2\pi f$. So R_{ct} can be obtained directly from Nyquist plots. C_p and R_p denote the pseudo-capacitance and pseudo-resistance, respectively, associated with the potential-dependent surface coverage of an adsorbed intermediate in the OER mechanism. These data exhibited similar features as those reported for Co [34], Ni [35], IrO_2 [36] and Co_3O_4 prepared by thermal decomposition on Ni substrates for OER [37]. The parameters R_{el} , R_{ct} , C_{dl} , C_p and R_p in Table 2 were calculated by a NLLS fit routine, in term of the geometric area. The simulated results (also shown in Fig. 9) exhibit good agreement with the experimental data. Among all of Co+Ni mixed oxides, the mixed oxide electrodeposited from $\text{Co}^{2+}/\text{Ni}^{2+} = 1:1$ solution, shows the lowest values of R_{ct} and R_p and exhibits the best catalytic performance for OER. The results from EIS are coherent to those obtained from CV and Tafel curve measurements.

4. Discussion

Co+Ni mixed oxides prepared by cycle potentiodynamic electrodeposition on Ni substrates are probably mixed oxides of cobalt and nickel, having different mixed phase structure. The mixed oxide electrodeposited from solution with $\text{Co}^{2+}/\text{Ni}^{2+} = 1:1$ has dominant spinel NiCo_2O_4 crystalline structure and largest real area, so exhibits best performance for oxygen evolution in alkaline media. Moreover, the all mixed Co+Ni

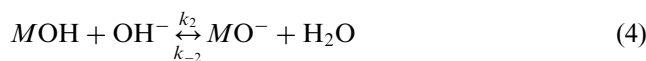
Table 2

Simulated parameters of the elements on equivalent circuits for oxygen evolution on Co+Ni mixed oxides electrodeposited from different $\text{Co}^{2+}/\text{Ni}^{2+}$ ratio solutions

$\text{Co}^{2+}/\text{Ni}^{2+}$	R_{el} ($\Omega \text{ cm}^2$)	C_{dl} (F cm^{-2})	R_{ct} ($\Omega \text{ cm}^2$)	C_p (F cm^{-2})	R_p ($\Omega \text{ cm}^2$)
Pure Co^{2+}	5.6	0.00275	29.3	0.00143	135.3
5:1	4.7	0.00258	26.8	0.00114	79.9
2:1	4.6	0.00263	13.4	0.00192	73.1
1:1	4.5	0.01770	4.2	0.01360	9.4
1:2	5.1	0.00925	30.0	0.00449	259.1
1:5	5.0	0.01368	43.2	0.01003	518.3

oxides with different composition have same mechanisms for oxygen evolution reaction. From polarization measurements performed in OER on all mixed oxides, OER was found to be governed by two Tafel regions, about 40 mV dec^{-1} at low overpotential and about 120 mV dec^{-1} at high overpotential in 1 M NaOH. At low and high overpotential, reaction order with respect to OH^- were found to be $p = 2$ and 1, respectively. Tafel slope close to 40 mV dec^{-1} can be attributed to the second electron transfer step being rate determining, while 120 mV dec^{-1} is usual due to the first electron reaction being rate determining. EIS measurements exhibit only one capacitive time constant related to the potential-dependent surface coverage. This denotes that only one adsorbed intermediate clearly exists in OER [38].

To explain the Tafel slope and reaction order to OH^- , as well as only one adsorbed intermediate, a simplified mechanism for the OER on Co+Ni mixed oxide electrodes is assumed.



Similar mechanisms involving the formation of a physisorbed hydrogen peroxide intermediate have been proposed on some other anodes also [39,40]. As demonstrated in [16], assuming the total surface coverage by adsorbed intermediates MOH under Langmuir adsorption conditions and applying quasi-equilibrium conditions to step (3), rate step determining to step (5), so that the surface coverage θ by MOH is

$$\theta = K_1 C_{\text{OH}^-} \exp(F\eta/RT), \quad (7)$$

where $K_1 (= k_1/k_{-1})$ is the equilibrium constant for the adsorption–desorption step (3). So, the overall current density for oxygen evolution can be given as:

$$j = 2FK_1 K_2 k_3 C_{\text{OH}^-}^2 \exp[(1 + \beta)F\eta/RT] \quad (8)$$

Eq. (8) gives a Tafel slope of 40 mV dec^{-1} at 25°C (assuming $\beta \approx 0.5$) and second order reaction in OH^- concentration.

However, with an increase of anodic potentials, the electrochemical rate for step (5) becomes so rapid that the rate of the overall reaction is controlled by step (3). Under this situation, the overall current density in low adsorption condition can be given as

$$j = 2FK_1 C_{\text{OH}^-} \exp[(\beta)F\eta/RT]. \quad (9)$$

Eq. (9) demonstrates a Tafel slope of 120 mV dec^{-1} and first-order kinetics in OH^- concentration. Thus, the rate law (8) and (9) explain well the experimentally determined electrode kinetic parameters. The existence of only one capacitive contribution in the impedance spectra, associated with the potential dependence of the surface concentration of the MOH intermediate.

5. Conclusion

A series of Co+Ni mixed oxides can be prepared on Ni substrate by anodic electrodeposition technique. The Co+Ni mixed oxides have different phase composition and surface structure with the variable Co contents. By electrochemical measurements, the electrodeposited mixed Co+Ni oxides exhibit good chemical stability and catalytic activity to oxygen evolution reaction in alkaline media. Especially the mixed oxide deposited from solution containing $\text{Co}^{2+}/\text{Ni}^{2+}$ ratio of 1:1, has dominant spinel type NiCo_2O_4 crystalline structure and large porosity surface, and exhibits the best catalytic performance for oxygen evolution.

The oxygen evolution kinetics on mixed Co+Ni oxides in alkaline solution was studied by means of steady-state polarization and EIS. The results indicate that all mixed Co+Ni oxides with different composition have similar kinetic mechanisms for oxygen evolution reaction. Two well-defined Tafel slopes, i.e., $40\text{--}48 \text{ mV dec}^{-1}$ at low overpotential region and $110\text{--}120 \text{ mV dec}^{-1}$ at high overpotential region were obtained. Moreover reaction orders with respect to OH^- on all mixed oxides at low and high overpotential are very close to 2.0 and 1.0, respectively. EIS measurements show that the OER is a multi-step reaction involving one intermediated species adsorbed at the oxide surface. According to a proposed reaction model, Tafel slope and a reaction order at different overpotential regions were explained by kinetic analysis and theoretical expressions.

Acknowledgment

This project was supported by China Postdoctoral Science Foundation.

Reference

- [1] S. Trasatti, *Electrochim. Acta* 29 (1984) 1503.
- [2] N.H. Ling, M. Prestat, J.L. Gautier, *Electrochim. Acta* 42 (1997) 197.
- [3] N. Noel, C. Ravichandran, P.N. Anantharaman, *J. Appl. Electrochem.* 25 (1995) 690.
- [4] A.C.C. Tseung, S. Jasem, *Electrochim. Acta* 22 (1977) 31.
- [5] S. Trasatti, *Electrochim. Acta* 36 (1991) 225.
- [6] R. Bertonecello, F. Furlanetto, P. Guerriero, M. Musiani, *Electrochim. Acta* 44 (1999) 4061.
- [7] S. Cattarin, P. Guerriero, M. Musiani, *Electrochim. Acta* 46 (2001) 4229.
- [8] M. Musiani, F. Furlanetto, P. Guerriero, *J. Electroanal. Chem.* 440 (1997) 131.
- [9] C.H. Comninellis, G.P. Vercesi, *J. Appl. Electrochem.* 21 (1991) 335.
- [10] B. Marsan, N. Fradette, G. Beaudoin, *J. Electrochem. Soc.* 139 (1992) 1889.
- [11] R.N. Singh, A.K. Singh, J.P. Singh, *Electrochim. Acta* 47 (2002) 3873.
- [12] L.C. Schumacher, I.B. Holzhueter, I.R. Hill, *Electrochim. Acta* 35 (1990) 975.
- [13] W.J. King, A.C.C. Tseung, *Electrochim. Acta* 19 (1974) 485.
- [14] R.N. Singh, M. Hamdani, J.F. Koenig, *J. Appl. Electrochem.* 20 (1990) 442.
- [15] V. Rashkova, S. Kitova, I. Konstantinov, T. Vitanov, *Electrochim. Acta* 47 (2002) 1555.
- [16] R.N. Singh, J.F. Koenig, G. Poillerat, P. Chartier, *J. Electrochem. Soc.* 137 (1990) 1408.
- [17] L.A. De Faria, M. Prestat, J.F. Koenig, P. Chartier, S. Trasatti, *Electrochim. Acta* 44 (1998) 1481.
- [18] M.R. Gennero de Chialvo, A.C. Chialvo, *Electrochim. Acta* 38 (1993) 2247.
- [19] C.C. Hu, Y.S. Lee, T.C. Wen, *Mater. Chem. Phys.* 48 (1997) 246.
- [20] I. Serebrennikova, V.I. Briss, *J. Electrochem. Soc.* 144 (1997) 566.
- [21] D. Tench, L.F. Warren, *J. Electrochem. Soc.* 130 (1983) 869.
- [22] Y.W.D. Chen, R.N. Noufi, *J. Electrochem. Soc.* 131 (1984) 1447.
- [23] I.G. Casella, *J. Electroanal. Chem.* 520 (2002) 119.
- [24] E.B. Castro, S.G. Real, L.F.P. Dick, *Int. J. Hydrogen Energy* 29 (2004) 255.
- [25] K. Izumiya, E. Akiyama, H. Abazaki, K. Hashimoto, *Electrochim. Acta* 43 (1998) 3303.
- [26] G. Milazzo, S. Caroli, *Tables of Standard Electrode Potentials*, Wiley, New York, 1978.
- [27] D. Baronetto, I.M. Kodintsev, S. Trasatti, *J. Appl. Electrochem.* 24 (1994) 189.
- [28] K. Lian, S.J. Thorpe, D.W. Kirk, *Electrochim. Acta* 37 (1992) 2029.
- [29] J. Haenen, W. Visscher, E. Barendrecht, *Electrochim. Acta* 31 (1986) 1541.
- [30] P. Rasiyah, A.C.C. Tseung, *J. Electrochem. Soc.* 130 (1983) 2384.
- [31] S.M. Jasem, A.C.C. Tseung, *J. Electrochem. Soc.* 126 (1979) 1353.
- [32] S.K. Tiwari, S. Samuel, R.N. Singh, *Int. J. Hydrogen Energy* 20 (1995) 9.
- [33] X. Nikolov, R. Darkaoui, E. Zhecheva, R. Stoyanova, *J. Electroanal. Chem.* 429 (1997) 157.
- [34] H. Willems, A.G.C. Kobustien, J.H.W. De Wit, G.H.J. Broers, *J. Electroanal. Chem.* 170 (1984) 227.
- [35] T. Osaka, Y. Yatsuda, *Electrochim. Acta* 29 (1984) 677.
- [36] L.A. Dasilva, V.A. Alves, M.A.P. Dasilva, S. Trasatti, *Electrochim. Acta* 42 (1997) 271.
- [37] B.E. Conway, T.C. Liu, *Ber. Bunsenges. Phys. Chem.* 91 (1987) 461.
- [38] T.C. Liu, B.E. Conway, *J. Appl. Electrochem.* 17 (1987) 983.
- [39] J. Kupka, A. Budniok, *J. Appl. Electrochem.* 20 (1990) 1015.
- [40] J. Sarowka, A. Budniok, B. Bzowski, J. Warczewsk, *Thin Solid Films* 307 (1997) 233.